Aggregation and Fibrillization of the Recombinant Human Prion Protein huPrP90−231†

Wieslaw Swietnicki, Manuel Morillas, Shu G. Chen, Pierluigi Gambetti, and Witold K. Surewicz*

Department of Pathology, Case Western Reserve University, Cleveland, Ohio 44106

Received August 20, 1999; Revised Manuscript Received October 27, 1999

ABSTRACT: According to the "protein-only" hypothesis, the critical step in the pathogenesis of prion diseases is the conformational transition between the normal (PrP^C) and pathological (PrP^{Sc}) isoforms of prion protein. To gain insight into the mechanism of this transition, we have characterized the biophysical properties of the recombinant protein corresponding to residues 90−231 of the human prion protein (huPrP90−231). Incubation of the protein under acidic conditions (pH 3.6−5) in the presence of 1 M guanidine-HCl resulted in a time-dependent transition from an α-helical conformation to a β-sheet structure and oligomerization of huPrP90−231 into large molecular weight aggregates. No stable monomeric β-sheet-rich folding intermediate of the protein could be detected in the present experiments. Kinetic analysis of the data indicates that the formation of β-sheet structure and protein oligomerization likely occur concomitantly. The β-sheet-rich oligomers were characterized by a markedly increased resistance to proteinase K digestion and a fibrillar morphology (i.e., they had the essential physicochemical properties of PrP^{Sc}). Contrary to previous suggestions, the conversion of the recombinant prion protein into a PrP^{Sc}-like form could be accomplished under nonreducing conditions, without the need to disrupt the disulfide bond. Experiments in urea indicate that, in addition to acidic pH, another critical factor controlling the transition of huPrP90−231 to an oligomeric β-sheet structure is the presence of salt.

Prion diseases are neurodegenerative disorders that affect animals and humans. In animals, the best known forms are scrapie in sheep and bovine spongiform encephalopathy in cattle, whereas the human variants include Creutzfeldt-Jakob disease, Gerstmann-Straussler-Scheinker disease, and fatal familial insomnia. The unique feature of these diseases is that, in addition to sporadic and inherited forms, they may be acquired by transmission of an infectious agent (*1*−*4*).

According to the "protein-only" hypothesis, the infectious prion pathogen consists of an abnormal prion protein, PrP^{Sc}[1] (*1*, *5*, *6*). This protein is an altered isoform of a normal cellular protein, PrP^C, that is host-encoded by a chromosomal gene and abundantly expressed in mammalian cells. PrP^C is a 209-residue glycoprotein that has a single disulfide bridge, two N-glycosylation sites, and a glycosyl phosphatidylinositol anchor (*7*). It is localized in cholesterol-rich membrane microdomains called rafts or caveo-like domains (*8*). The covalent structure of PrP^{Sc} is most likely identical with that of PrP^C (*7*, *9*). However, the two prion protein isoforms have profoundly different physical properties. PrP^C exists as a monomer that is readily degradable by proteinase K, whereas PrP^{Sc} forms insoluble aggregates that show high resistance to proteinase K digestion and often have the characteristics of an amyloid (*10*−*13*). Furthermore, in contrast to a largely α-helical structure of PrP^C, the PrP^{Sc} isoform is characterized by a high content of β-sheet structure (*14*−*17*).

The conformational transition of PrP^C whereby some α-helices are converted to an oligomeric β-sheet structure is believed by many to constitute a critical step in the pathogenesis of prion disorders (*1*). A key to understanding the molecular mechanism of the PrP^C to PrP^{Sc} conversion is to determine the folding pathway and aggregation properties of the prion protein. In this study, we have explored the biophysical properties of the recombinant protein corresponding to residues 90−231 of the human prion protein (huPrP90−231). According to the NMR data, the recombinant prion protein contains a well-structured core domain (residues 125−231) consisting of three α-helices and two short β-strands, whereas the N-terminal part of the molecule is highly flexible and largely unordered (18−20). The 90−231 region of the prion protein is of special interest, since it encompasses the entire sequence of the proteinase K-resistant core of PrP^{Sc}, contains all point mutations associated with hereditary human prion disorders, and is sufficient for the propagation of the disease (*1*, *4*). Our data shows that, under appropriate solvent conditions, huPrP90−231 spontaneously converts to an oligomeric form with the physicochemical properties very similar to those of PrP^{Sc}. We also demonstrate that, contrary to previous suggestions (*21*), the recombinant prion protein may acquire the PrP^{Sc}-like properties without the need to reduce the disulfide bond. These findings provide a new insight into the mechanism of the conversion between the normal and pathogenic forms of prion protein.

† This work was supported by National Institutes of Health grant NS38604 (to W.K.S.).

* To whom correspondence should be addressed: Department of Pathology, Case Western Reserve University, 2085 Adelbert Road, Cleveland, OH 44106. Telephone: 216-368-0139. Fax: 216-368-2546. E-mail: wks3@pop.cwru.edu.

[1] Abbreviations: PrP, prion protein; PrP^{Sc}, scrapie PrP isoform; PrP^C, cellular PrP isoform; huPrP90−231, recombinant human prion protein fragment 90−231; NMR, nuclear magnetic resonance; CD, circular dichroism; GdnHCl, guanidine hydrochloride.

10.1021/bi991967m CCC: $19.00
Published on Web 12/14/1999

MATERIALS AND METHODS

Plasmid Construction. cDNA coding for the N-terminally truncated human prion protein (huPrP90−231) was amplified from a plasmid pVZ21 (*22*) by PCR using primers 5′-CAT GGT GGT *GGA TCC* GGG TCA AGG AGG and 5′-GAG GAT CGA GCT GA*G AAT TC*C TCT CCA CCT G. After digestion with *Eco*RI and *Bam*HI enzymes (restriction sites indicated in italics), the amplified cDNA and a double stranded linker coding for the thrombin cleavage site (5′-P-CT AGC CTG GTT CCG CGT GGT TCG and 5′- P-G ATC CGA ACC ACG CGG AAC CAG G) were ligated into a pRSET B vector (Invitrogen) that was predigested with *Nhe*I and *Eco*RI enzymes. The final construct coded for huPrP90−231 fused to an N-terminal linker containing 6xHis tail and a thrombin cleavage site. A GSDP fusion at the N-terminus remained after thrombin cleavage of the linker. All DNA manipulations were carried out according to standard protocols (*23*). DNA sequence of the construct was verified by automated DNA sequencing at the Case Western Reserve University Molecular Biology Core Facility.

Protein Expression and Purification. Protein was expressed and purified as described previously (*24*), with the exception that the His tail was cleaved by 4 h treatment at room temperature with 10 units thrombin/mg protein (10 mM potassium phosphate, pH 6.4) and subsequent ion exchange chromatography was performed on a CM Sepharose column (Pharmacia) using a linear 0−500 mM gradient of NaCl in 10 mM phosphate, pH 6.4. The purity of the final product was better than 95% as judged by SDS-polyacrylamide gel electrophoresis. The identity of the protein was further confirmed by mass spectrometry. Formation of the disulfide bond was verified by the lack of free thiol groups in the unfolded protein, as determined by the inaccessibility of cysteine residues to derviatization with iodoacetic acid. Protein concentration was determined spectrophotometrically using the molar extinction coefficient, ϵ_{276}, of 21 640 M^{-1} cm^{-1}.

Spectroscopic Measurements. Far-UV circular dichroism spectra were obtained on a Jasco J-600 spectropolarimeter at room temperature. The measurements were performed in a 0.2 mm or 1 mm path length cylindrical cell. Light angle light scattering experiments were performed at 400 nm using an SLM 8100 spectrofluorometer.

Size-Exclusion Chromatography. Size-exclusion chromatographic measurements were performed using the FPLC system equipped with a Superose 6 10/30 HR gel filtration column (Pharmacia). Before each run, the column was preequilibrated with at least five column volumes of the elution buffer. A typical flow rate was 0.35 mL/min, and the elution of protein from the column was monitored by measuring absorbance at 280 nm. Calibration of the column was performed using molecular weight standards for size exclusion chromatography (Sigma).

Proteinase K Sensitivity. A sample of huPrP90−231 (0.4 mg/mL) was preincubated for 24 h with or without GdnHCl in 50 mM sodium acetate, pH 4.0. The protein was then transferred to the digestion buffer (1 mM EDTA, 0.05% sodium deoxycholate, 50 mM sodium acetate, pH 4) containing various concentrations of proteinase K (0−50 μg/mL) and incubated for 1 h at 37 °C. The digestion reaction was terminated by addition of Pefabloc (Boehringer Mannheim) to a final concentration of 3 mM. After the sample was boiled in a loading buffer (3% SDS, 3% β-mercaptoethanol, 2 mM EDTA, 62.5 mM Tris, pH 6.8), protein fragments were separated by SDS-polyacrylamide gel electrophoresis and transferred onto an Immobilon P membrane (Millipore) for Western blot analysis. Prion protein was detected by 3F4 antibody (*25*) using the enhanced chemiluminescence kit (Amersham). In control experiments with other proteins, it was verified that proteinase K in the presence of 1 M GdnHCl retained its proteolytic activity.

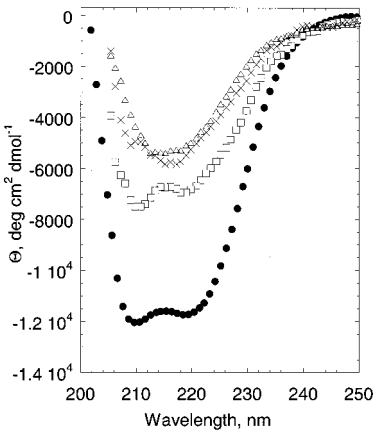

FIGURE 1: Time-dependent changes in far-UV circular dichroism spectrum of huPrP90−231 in the presence of 1 M GdnHCl at pH 4.0. The spectra shown were recorded 2 min (□), 40 min (×), and 90 min (Δ) after the addition of GdnHCl. Trace (●) represents the spectrum of the protein at pH 4.0 in the GdnHCl-free buffer. The concentration of the protein in each case was 0.4 mg/mL.

Electron Microscopy. For electron microscopy studies, protein solution (0.4 mg/mL) was preincubated for 24 h at room temperature in a buffer (10 mM sodium acetate, pH 4.0), containing 0.5 or 1 M GuHCl. A drop of each sample was placed on a carbon-coated EM grid (Electron Microscopy Sciences) and negatively stained with 2% (w/v) aqueous uranyl acetate. As a control, a sample of huPrP90−231 in the absence of the denaturant was prepared by the identical method. Grid preparations were visualized using a JEOL 100CX transmission microscope operating at 80 keV.

RESULTS

pH-Dependent Conformation of huPrP90−231 in 1 M GdnHCl. In the previous study, we showed that low concentrations of GdnHCl at acidic pH induce a transition in PrP90−231 from an α-helix to a β-sheet structure (*26*). To gain insight into the mechanism of this pH-dependent conformational transition, herein we have performed more detailed biophysical studies with the recombinant prion protein.

Figure 1 shows far-UV CD spectra of huPrP90−231 in 1 M GdnHCl, pH 4.0, as a function of time. In the absence of the denaturant, the spectrum has a double minimum at 222 and 208 nm and is characteristic of an α-helical structure (*27*). Upon addition of 1 M GdnHCl, there was a time-dependent decrease in the negative ellipticity, concomitant with a change in the shape of the spectrum to the one characteristic of proteins rich in β-sheet structure (minimum at approximately 215 nm). The spectral changes described above were highly reproducible (all results reported in this

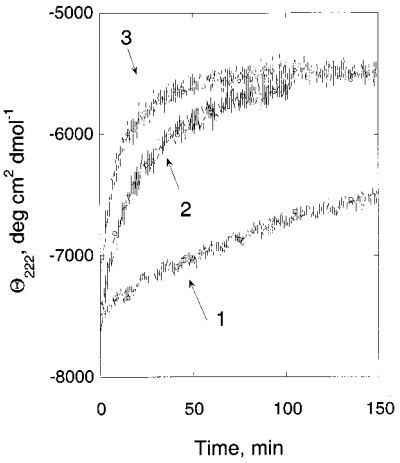

FIGURE 2: Time course of changes in the ellipticity at 222 nm for huPrP90−231 in the presence of 1 M GdnHCl at pH 3.6 (trace 3), 4.0 (trace 2), and 4.4 (trace 1). The concentration of the protein was 0.4 mg/mL.

study are based on at least three independent experiments). Quantitative determination of protein secondary structure in the presence of GdnHCl was, however, not feasible, since absorption of the denaturant precluded CD measurements below 205 nm.

To study the kinetics of the transition from α-helix to a *β*-sheet-rich conformation under different experimental conditions, we followed the time course of the decrease in the negative ellipticity at 222 nm, Θ_{222} (Figure 2). At pH between 3.6 and 4.4, the initial very rapid drop in Θ_{222} (that occurred within the 30 s dead-time of the experiment) was followed by a much slower phase. The rapid event most likely represents partial unfolding of the (presumably monomeric) protein. The above assignment of the rapid phase is consistent with recent data showing that the unfolding of mouse PrP121−231 in vitro is extremely fast, occurring on the time scale of milliseconds (*28*). The slow phase, on the other hand, is concomitant with changes in the shape of the spectrum to the one characterized by a single minimum around 215 nm (see Figure 1). Therefore, this phase appears to represent the formation of a *β*-sheet structure. The interpretation of the kinetic traces at highly acidic pH is strongly supported by data obtained at pH 5. Under the latter conditions, 1 M GdnHCl is insufficient to significantly unfold the protein (*26*). Therefore, consistent with our interpretation, only a slow phase (corresponding to the helix to *β*-sheet transition) could be seen in the Θ_{222} versus time plot at pH 5 (see Figure 3 and the discussion below).

Data of Figure 2 shows that the time course of the GdnHCl-induced helix to *β*-sheet transition in huPrP90−231 is strongly pH dependent. Under highly acidic conditions and with a protein concentration used in this experiment (0.4 mg/mL), the conformational change was relatively fast, occurring within less than 1 h at pH 3.6 and approximately 2 h at pH 4.0. Raising the pH to 4.4 dramatically slowed the reaction; the transition to a *β*-sheet structure was completed only after approximately 1 day of incubation. Upon further reduction of acidity to pH 5, the formation of a *β*-sheet structure could be observed only after increasing the concentration of huPrP90−231. As shown in Figure 3, at pH 5 and with a protein concentration of 1.6 mg/mL, the spectral changes characteristic of α-helix to *β*-sheet transition

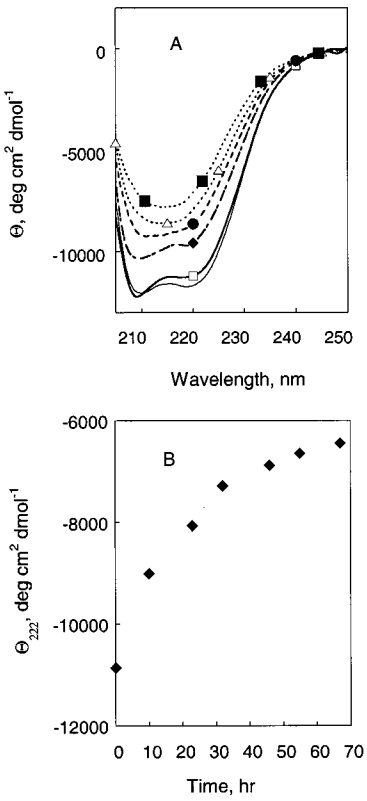

FIGURE 3: A transition of huPrP90−231 to a *β*-sheet conformation in the presence of 1 M GdnHCl at pH 5.0. Panel A: Far-UV circular dichroism spectra of the protein in the absence of GdnHCl (no symbol) and recorded 2 min (□), 10 h (♦), 23 h (●), 32 h (△) and 67 h (■) after the addition of GdnHCl. Panel B: The kinetics of changes in ellipticity at 222 nm. The concentration of huPrP90−231 was 1.6 mg/mL.

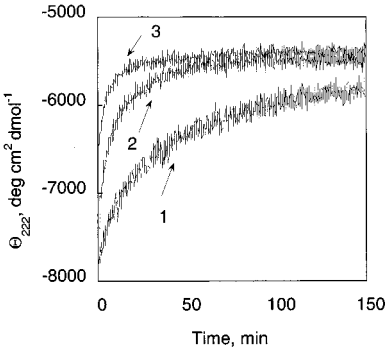

FIGURE 4: Time dependence of ellipticity at 222 nm for huPrP90−231 in 1 M GdnHCl, pH 4.0, at protein concentration of 0.2 (trace 1), 0.4 (trace 2), and 0.8 mg/mL (trace 3). GdnHCl was added to protein solution at time zero. After 24 h incubation, the spectra at each protein concentration showed a minimum at 215 nm and were characteristic of a *β*-sheet structure.

occurred within tens of hours (half-time of approximately 20 h). No *β*-sheet structure formation was observed under the conditions of neutral pH: the CD spectrum of huPrP90−231 at pH 7 retained the α-helical character even after two weeks of incubation in the presence of 1 M GdnHCl (data not shown for brevity).

The kinetics of α-helix to *β*-sheet transition in huPrP90−231 at a given pH was strongly dependent on the protein concentration. A representative set of kinetic traces for huPrP90−231 at pH 4.0 is shown in Figure 4. Clearly, the reaction becomes faster as the concentration of the protein is increased. The above concentration dependence strongly

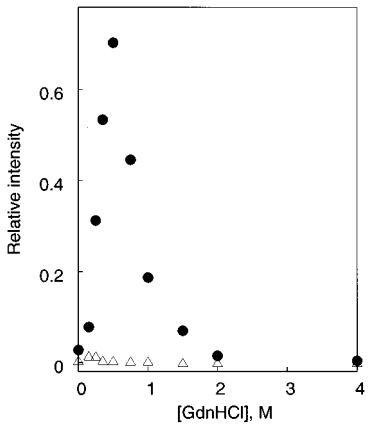

FIGURE 5: Right angle light scattering of huPrP90−231 in GdnHCl at pH 4.0 (●) and 7.0 (△). Before measurements, samples of the protein at each GdnHCl concentration were incubated for 24 h. The concentration of huPrP90−231 was 0.4 mg/mL.

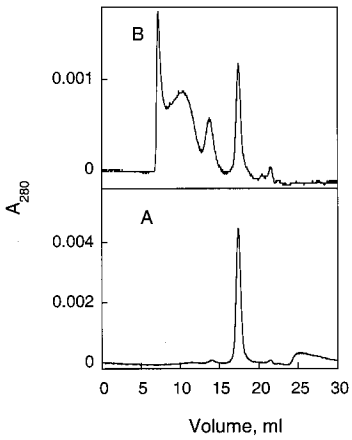

FIGURE 6: Time-dependent oligomerization of huPrP90−231 in 1 M GdnHCl, pH 4.0, as monitored by size exclusion chromatography. The chromatographs shown represent elution profiles for the protein following 2 (A) and 120 min (B) of incubation in the presence of GdnHCl. The concentration of huPrP90−231 was 0.4 mg/mL.

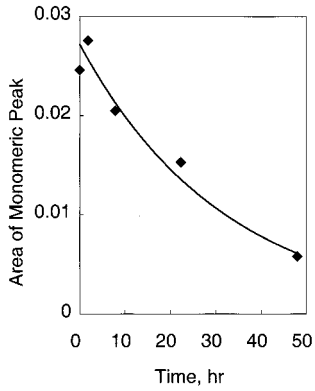

FIGURE 7: The kinetics of huPrP90−231 oligomerization in 1 M GdnHCl at pH 5.0 as monitored by size exclusion chromatography. The area of the peak corresponding to the monomeric protein is plotted as a function of preincubation time in 1 M GdnHCl. The concentration of huPrP90−231 was 1.6 mg/mL.

suggests that the formation of β-sheet structure in huPrP90−231 may be associated with the oligomerization of the protein.

Aggregation State of huPrP90−231 in the Presence of GdnHCl. The aggregation state of the β-sheet-rich form of huPrP90−231 was initially assessed by right angle light scattering. Although under the present experimental conditions the solution of huPrP90−231 always appeared transparent to the eye, light scattering measurements indicate that at acidic pH the protein undergoes GdnCl-dependent oligomerization. Figure 5 shows the intensity of the scattered light following 24 h incubation of huPrP90−231 (0.4 mg/mL) at pH 4 in the presence of increasing concentrations of GdnHCl. The scattered light reached a maximum at approximately 0.5 M GdnCl and gradually decreased upon further increase of the concentration of the chaotropic salt. However, at 1 M GdnHCl the intensity of light scattering still remained 60-fold higher than that of the protein solution in a GdnHCl-free buffer. The effect described above was observed only under acidic conditions: no increase in light scattering was found upon incubation of huPrP90−231 with GdnHCl at pH 7 (Figure 5).

More detailed information about the aggregation state of the prion protein was obtained by size exclusion chromatography. In the absence of GdnHCl, huPrP90−231 at pH between 7 and 4 eluted at a time corresponding to a globular protein with a molecular weight of approximately 20 kDa. A slightly higher apparent molecular mass than expected for huPrP90−231 monomer may be explained by the presence of an unstructured N-terminal region in the protein (*19*, *20*). A monomeric state of the protein under these conditions was further confirmed by quasi-elastic light scattering measurements (data not shown for brevity). At pH 7, even prolonged incubation with 1 M GdnHCl did not change the elution profile of the protein. A markedly different behavior was observed under acidic conditions. The elution profile of huPrP90−231 at pH 4.0 obtained immediately after addition of 1 M GdnHCl indicates the presence of a predominant monomeric species (Figure 6 A). However, following 2 h incubation in the presence of 1 M GdnHCl, only approximately 20% of huPrP90−231 retained the monomeric structure, whereas the vast majority of the protein eluted as high molecular weight aggregates (Figure 6B). The size of these oligomeric species varied between approximately 400 and 2000 kDa. The aggregates grew with time, and after few days, their size was beyond the fractionation limit of the column (about 4×10^7 Da for globular proteins). The aggregation process was apparently irreversible as neutralization of the solution did not restore the monomeric protein.

At pH 4, the aggregation of huPrP90−231 in the presence of 1 M GdnHCl was too fast to allow a quantitative kinetic analysis by size exclusion chromatography. However, the rate of protein oligomerization was markedly reduced upon increasing the pH to 5. Under such conditions, it was possible to follow the kinetics of oligomer formation and compare it with the time-course of GdnCl-induced changes in the CD spectra of the protein. Figure 7 shows the area of the chromatographic peak corresponding to the PrP90−231 monomer at pH 5 as a function of preincubation time in the presence of 1 M GdnHCl (protein concentration of 1.6 mg/mL). A comparison of this curve with the CD data of Figure 3 indicates the time-course of protein oligomerization and that of α-helix to β-sheet transition are very similar. The estimated half-times for huPrP90−231 oligomerization (loss of the monomeric species) and β-sheet formation are 22 and 20 h, respectively.

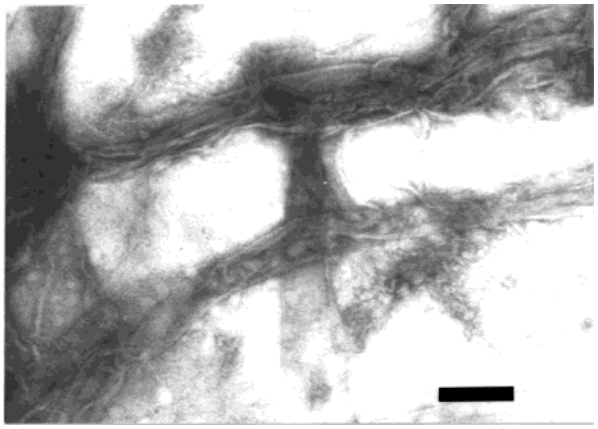

FIGURE 8: Electron micrograph taken following 24 h of incubation of huPrP90−231 (0.4 mg/mL) in the presence of 1 M GdnHCl at pH 4.0. In addition to the fibrillar structures shown in the micrograph, numerous amorphous aggregates were also observed. The fibrillar and amorphous structures segregated in different parts of the grid; only the fibril-rich field is shown. The bar corresponds to 250 nm.

The β-sheet-rich aggregates formed in the presence of GdnHCl were thioflavin T positive, as indicated by the increased fluorescence intensity at 485 nm of the dye in the presence of the aggregated (but not monomeric) protein (data not shown for brevity). Binding of thioflavin T suggests that the aggregates formed by huPrP90−231 have amyloid-like character (*29*). The morphology of these aggregates was further studied by electron microscopy. The micrographs of the protein incubated at pH 4 with 0.5 or 1 M GdnHCl showed numerous fibrillar filaments (Figure 8). The fibrils were about 15 nm in diameter and of variable length. In addition to the fibrillar structures, amorphous aggregates of irregular shape were also observed. These two types of morphologies usually segregated in different parts of the grid (only the fibril-rich field is shown in Figure 8).

Proteinase K Resistance. Aggregation of huPrP90−231 was accompanied by a substantial increase in the resistance of the protein to proteinase K digestion. As shown in Figure 9, treatment of a monomeric huPrP90−231 with more than 1 μg/mL of proteinase K resulted in a complete degradation of the protein. However, preincubation of huPrP90−231 under the conditions promoting formation of an oligomeric β-sheet structure (pH 4; 0.5 or 1 M GdnHCl) rendered the protein resistant to the degradation in the presence of as much as 10 μg/mL of proteinase K.

Conformation and Aggregation State of huPrP90−231 in the Presence of Urea and NaCl. It was recently reported that the C-terminal fragment of mouse PrP corresponding to the folded domain (residues 121−231) forms a β-sheet structure upon partial unfolding in 3.5−4 M urea under the conditions of acidic pH (*30*). To test if urea is also able to induce the α-helix to β-sheet transition in a physiologically more relevant longer variant of prion protein, we performed a series of circular dichroism experiments with huPrP90−231. As shown in Figure 10A, the CD spectrum of huPrP90−231 following up to 8 days incubation in 50 mM sodium acetate containing 3.5 M urea and buffered to pH 4, has a minimum at 208 nm and a well defined shoulder around 220 nm. The above spectrum is characteristic of a partially unfolded protein, but not of a β-sheet structure. However, a time-dependent transition to a spectrum characteristic of a

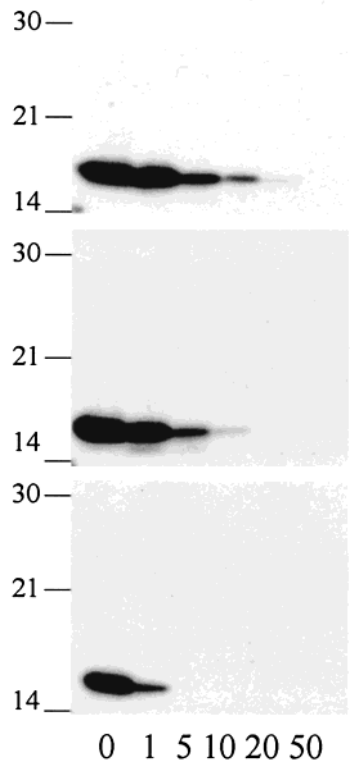

FIGURE 9: Proteinase K resistance of huPrP(23−231) following 24 h of incubation at pH 4.0 in the absence (bottom panel) and presence of 1 M GdnHCl (middle panel) and 0.5 M GdnHCl (top panel). Approximate molecular weights in kDa are shown on the left and the concentration of proteinase K in μg/mL is indicated below each lane.

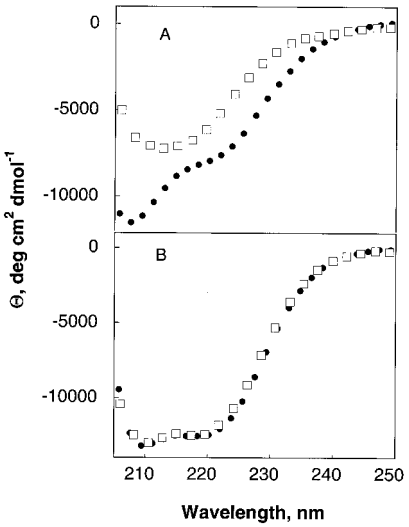

FIGURE 10: Far-UV circular dichroism spectra of huPrP90−231 in 3.5 M urea. Panel A: Protein was incubated for 48 h in the pH 4.0 buffer containing 3.5 M urea and no NaCl (●) or 150 mM NaCl (□). The spectra remained unchanged upon further incubation of the protein up to 8 days. Panel B: Protein was incubated for 48 h in the pH 7.0 buffer containing 3.5 M urea and no NaCl (●) or 150 mM NaCl (□). The concentration of protein in each case was 1 mg/mL.

β-structure could be observed upon incubation of huPrP90−231 in the same buffer containing 150 mM sodium chloride (Figure 10 A). The above transition occurred only at acidic pH; the CD spectrum of the protein incubated for up to 8 days in 3.5 M urea, 150 mM NaCl at pH 7 retained the α-helical character (Figure 10B).

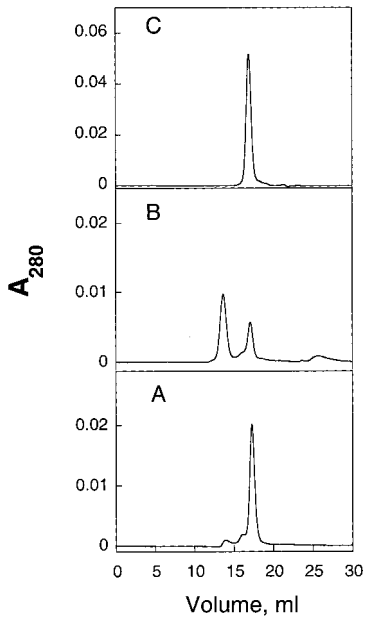

FIGURE 11: Size exclusion chromatography profiles for huPrP90−231 following preincubation in 3.5 M urea, 150 mM NaCl, pH 4.0, for 2 min (A) and 40 h (B). Panel C represents the elution profile of the protein incubated for 8 days in 3.5 M urea, 150 mM NaCl at pH 7.2. The concentration of the protein in each case was 1 mg/mL.

In addition to causing a transition to a β-sheet conformation, incubation of huPrP90−231 under acidic conditions in the presence of urea and sodium chloride also resulted in a time-dependent protein oligomerization (Figure 11). The aggregates formed under these conditions were characterized by a relatively uniform size of approximately 400 kDa. No detectable oligomerization of the protein was found in the same solvent at neutral pH (Figure 11C).

DISCUSSION

According to the "protein-only" hypothesis, the key molecular event in the pathogenesis of prion disease is the conversion of prion protein from an α-helical conformation of PrP^{C} into the oligomeric β-sheet-rich structure of PrP^{Sc} (*1*, *2*, *4*, *6*). In this context, it is not surprising that studies aimed at understanding the structural and biophysical properties of PrP have recently emerged as a central theme in prion research. Since it is very difficult to obtain sufficient amounts of highly purified protein from the brain, the biophysical studies have relied largely on the recombinant prion protein expressed in bacterial systems (*24*, *26*, *31*−*33*). Although the recombinant PrP lacks glycosylation and the glycosyl phosphatidylinositol anchor, its secondary and tertiary structure appear to be very similar to that of brain PrP^{C} (*34*). This protein provides a very useful model for studying the physicochemical properties and conformational transitions of the prion protein (*18*−*21*, *26*, *28*, *30*, *31*, *33*−*36*).

In the previous study, we showed that in the presence of relatively low concentrations of GdnHCl under acidic conditions, huPrP90−231 undergoes a major transition from an α-helical conformation to a β-sheet structure (*26*). A similar transition was also reported for mouse PrP121−231 upon incubation at acidic pH in the presence of urea (*30*). Preliminary data suggested that the β-sheet-rich conformer of huPrP90−231 in GdnHCl (or mouse PrP121−231 in urea) represents a stable monomeric folding intermediate of the prion protein (*26*, *30*). It was also postulated that this intermediate may exemplify a prototype of a soluble (monomeric) precursor of PrP^{Sc}. However, the present data, which provides a more detailed insight into the mechanism of conformational transitions of huPrP90−231, calls for a reevaluation of some of the conclusions of the previous study.

One of the main findings of this study is the demonstration that the GdnHCl/acidic pH-induced transition of huPrP90−231 to a β-sheet-rich structure is invariably accompanied by protein self-association into large molecular weight aggregates. The question remains: which of these two events occur first. Although the kinetics of the transition to a β-sheet structure and that of protein aggregation appear to be very similar, the relatively low time-resolution of the present experiments does not allow us to eliminate the possibility that the oligomerization of huPrP90−231 may be preceded by the formation of a monomeric β-sheet-rich conformer. However, such a mechanism is rather unlikely in view of a strong dependence of the rate of conformational changes in huPrP90−231 on the protein concentration. The observed increase in the rate of β-sheet formation with increasing concentration of huPrP90−231 strongly suggests an alternative scenario in which the α-helix to β-sheet transition occurs simultaneously with protein oligomerization. The GdnHCl denaturation curves for huPrP90−231 and hamster PrP90−231 at low pH have previously been interpreted according to the three-state model that assumes the presence of a stable (monomeric) protein folding intermediate (*26*, *33*). However, the above interpretation has to be revised. Given the present data, the species previously assigned as an "equilibrium-folding intermediate" of huPrP90−231 appears to represent a β-sheet-rich oligomer rather than a monomeric protein. This finding does not preclude the possibility that prion protein may form monomeric folding intermediates. However, the present results indicate that any potential monomeric intermediate(s) that may occur during GdnHCl-induced denaturation of huPrP90−231 at acidic pH would be short-lived and highly prone to aggregation.

The conformational properties of huprP90−231 were also studied in the presence of a nonionic denaturant urea. Previous experiments indicate that in the presence of 3.5−4 M urea at acidic pH, the structure of the recombinant mouse PrP121−231 is characterized by a high content of β-sheet (*30*). Therefore, it was surprising that no transition to a β-sheet-rich conformer could be detected for huPrP90−231 in a low ionic strength buffer (pH 4) containing 3.5 M urea. Such a transition occurred, however, when the buffer was supplemented with sodium chloride. In analogy with the behavior of huPrP90−231 in GdnHCl, the α-helix to β-sheet transition in the urea/NaCl-containing buffer was accompanied by protein oligomerization. These data strongly suggests that the combination of acidic pH with partial protein unfolding is insufficient to induce the transition of huPrP90−231 to an oligomeric β-sheet structure. An additional factor required for the above transition is the presence of an appropriate salt. A critical role of ionic species in controlling the oligomerization state of the prion protein is further suggested by the preliminary observation that, at acidic pH, NaCl alone (i.e., in the absence of any denaturant) can induce aggregation of huPrP90−231. However, the latter aggregates appear to be different from those formed in the presence of

GdnHCl as they rapidly precipitate and show no fibrillar morphology.[2]

It is remarkable that the huPrP90−231 oligomer formed in the presence of GdnHCl is characterized not only by a β-sheet structure but also by an amyloid-like morphology and an increased resistance to proteinase K digestion (i.e., it has the essential physicochemical properties of PrP^{Sc} from the diseased brain). Furthermore, it should be noted that the PrP^{Sc}-like conformation of the recombinant PrP could be acquired only under the conditions of acidic pH. The behavior of prion protein at low pH is of particular interest and relevance in the context of prion disease pathogenesis. Although the precise subcellular localization of PrP^{Sc} propagation is a matter of controversy, substantial evidence indicates that the formation of brain PrP^{Sc} occurs in acidic compartments along the endocytic pathway (*37*, *38*). Thus, the present experimental system provides a physiologically relevant model for studying the physicochemical mechanisms of the PrP^{C} to PrP^{Sc} conversion. This model may also prove applicable for studying the mode of action of potential drugs, especially those designed to inhibit the α-helix to β-sheet transition in prion protein.

It should be noted that the conversion of huPrP90−231 into fibrillar aggregates was reported in a very recent study of Jackson et al. (*21*). However, these experiments were performed under the conditions resulting in the reduction of a single disulfide bond in the prion protein. It was also suggested that the reduced monomeric β-sheet form of huPrP90−231 constitutes an important precursor of amyloid-like fibrils. The present data clearly demonstrates that the reducing environment is not a prerequisite for the transition of the recombinant prion protein to a PrP^{Sc}-like form since huPrP90−231 can be converted into fibrillar, proteinase K-resistant structures under the conditions, that fully preserve the disulfide bridge. Furthermore, under nonreducing conditions, we find no evidence that a long-lived monomeric β-sheet form of huPrP90−231 is an essential intermediate on the pathway towards formation of the β-sheet rich oligomer. The finding that a reducing environment is not required for the transition of the recombinant prion protein into the scrapie-like form is of physiological significance since the authentic PrP^{Sc} is characterized by an intact disulfide bond (*39*). Furthermore, preservation of the disulfide bridge appears to be important for the infectivity of the prion protein (*40*) as well as for the PrP^{Sc}-induced conversion of PrP^{C} to the protease-resistant state in a cell-free system (*41*). It should be also noted that, consistent with the present data, the PrP^{Sc}-dependent conversion reaction in a cell-free system was found to be promoted by the presence of GdnHCl or physiological salts (*42*, *43*).

In conclusion, biophysical data presented here show that, under mildly denaturing conditions, the recombinant prion protein can be converted into an oligomeric β-sheet-rich form with physicochemical properties very similar to those of PrP^{Sc}. The key requirements for this transition are acidic pH and the presence of salt, but not necessarily the disruption of the disulfide bridge. These findings provide a rationale for the use of the recombinant prion protein as a model for studying the mechanism of PrP^{C} to PrP^{Sc} conversion.

[2] Morillas, M., Swietnicki, W., and Surewicz, W. K., unpublished data.

REFERENCES

1. Prusiner, S. B. (1998) *Proc. Natl. Acad. Sci. U.S.A. 95*, 13363−13368.
2. Weissman, C. (1996) *FEBS Lett. 389*, 3−11.
3. Gajdusek, D. C. (1977) *Science 197*, 943−960.
4. Parchi, P., Gambetti, P., Picardo, P., and Ghetti, B. (1998) in *Progress in Pathology IV* (Haddock, G. M., Ed.) pp 39−77, Churchill Livingstone, Edinburgh, UK.
5. Griffith, J. S. (1967) *Nature 215*, 1043−1044.
6. Prusiner, S. B. (1982) *Science 216*, 136−144.
7. Stahl, N., and Prusiner, S. B. (1991) *FASEB J. 5*, 2799−2807.
8. Vey, M., Pilkuhn, S., Wille, H., Nixon, R., DeArmond, S. J., Smart, E. J., Anderson, R. G. W., Taraboulos, A., and Prusiner, S. B. (1996) *Proc. Natl. Acad. Sci. U.S.A. 93*, 14945−14949.
9. Stahl, N., Baldwin, M. A., Teplow, D. B., Hood, L., Gibson, B. W., Burlingame, A. L., and Prusiner, S. B. (1993) *Biochemistry 32*, 1991−2002.
10. Meyer, R. K., McKinley, M. P., Bowman, K. A., Braunfeld, M. B., Barry, R. A., and Prusiner, S. B. (1986) *Proc. Natl. Acad. Sci. U.S.A. 83*, 2310−2314.
11. Oesch, B., Westaway, D., Walchli, M., McKinley, M. P., Kent, S. B., Aebersold, R., Barry, R. A., Tempst, P., Teplow, D. B., Hood, L. E., Prusiner, S. B., and Weissmann, C. (1985) *Cell 40*, 735−746.
12. McKinley, M. P., Meyer, R. K., Kenaga, L., Rahbar, F., Cotter, R., Serban, A., and Prusiner, S. B. (1991) *J. Virol. 65*, 1340−1351.
13. Prusiner, S. B., McKinley, M. B., Bowman, K. A., Bolton, D. C., Bendheim, P. E., Groth, D. E., and Glenner, G. G. (1983) *Cell 35*, 349−358.
14. Pan, K. M., Baldwin, M., Nguyen, J., Gasset, M., Serban, A., Groth, D., Mehlhorn, I., Huang, Z., Fletterick, R. J., Cohen, F. E., and Prusiner, S. B. (1993) *Proc. Natl. Acad. Sci. U.S.A. 90*, 10962−10966.
15. Caughey, B. W., Dong, A., Bhat, K. S., Ernst, D., Hayes, S. F., and Caughey, W. S. (1991) *Biochemistry 30*, 7672−7680.
16. Gasset, M., Baldwin, M. A., Fletterick, R. J., and Prusiner, S. B. (1993) *Proc. Natl. Acad. Sci. U.S.A. 90*, 1−5.
17. Safar, J., Roller, P. P., Gajdusek, D. C., and Gibbs, C. J., Jr. (1993) *Protein Sci. 2*, 2206−2216.
18. Riek, R., Hornemann, S., Wider, G., Billeter, M., Glockshuber, R., and Wuthrich, K. (1996) *Nature 382*, 180−182.
19. Donne, D. G., Viles, J. H., Groth, D., Mehlhorn, I., James, T. L., Cohen, F. E., Prusiner, S. B., Wright, P. E., and Dyson, H. J. (1997) *Proc. Natl. Acad. Sci. U.S.A. 94*, 13452−13457.
20. Liu, H., Farr-Jones, S., Ulyanov, N. B., Llinas, M., Marqusee, S., Groth, D., Cohen, F. E., Prusiner, S. B., and James, T. L. (1999) *Biochemistry 38*, 5362−5377.
21. Jackson, G. S., Hosszu, L. L., Power, A., Hill, A. F., Kenney, J., Saibil, H., Craven, C. J., Waltho, J. P., Clarke, A. R., and Collinge, J. (1999) *Science 283*, 1935−1937.
22. Petersen, R. B., Parchi, P., Richardson, S. L., Urig, C. B., and Gambetti, P. (1996) *J. Biol. Chem. 271*, 12661−12668.
23. Sambrook, J., Fritsch, E. F., and Maniatis, T. (1989) *Molecular Cloning: A Laboratory Manual*. Vols. 1−3, Cold Spring Harbor Laboratory, Cold Spring Harbor, NY.
24. Zahn, R., von Schroetter, C., and Wuthrich, K. (1997) *FEBS Lett. 470*, 400−404.
25. Kascsak, R. J., Rubenstein, R., Merz, P. A., Tonna-DeMasi, M., Fersko, R., Carp, R. I., Wisniewski, H. M., and Diringer, H. (1987) *J. Virol. 61*, 3688−3693.
26. Swietnicki, W., Petersen, R., Gambetti, P., and Surewicz, W. K. (1997) *J. Biol. Chem. 272*, 27517−27520.
27. Yang, J. T., Wu, C. S., and Martinez, H. M. (1986) *Methods Enzymol. 130*, 208−269.
28. Wildegger, G., Liemann, S., and Glockshuber, R. (1999) *Nat. Struct. Biol. 6*, 550−553.
29. LeVine, H. (1993) *Protein Sci. 2*, 404−410.
30. Hornemann, S., and Glockshuber, R. (1998) *Proc. Natl. Acad. Sci. U.S.A. 95*, 6010−6014.
31. Hornemann, S., and Glockshuber, R. (1996) *J. Mol. Biol. 261*, 614−619.

32. Hornemann, S., Korth, C., Oesch, B., Riek, R., Wider, G., Wuthrich, K., and Glockshuber, R. (1997) *FEBS Lett. 413*, 277−281.
33. Zhang, H., Stockel, J., Mehlhorn, I., Groth, D., Baldwin, M. A., Prusiner, S. B., James, T. L., and Cohen, F. E. (1997) *Biochemistry 36*, 3543−3553.
34. Stockel, J., Safar, J., Wallace, A. C., Cohen, F. E., and Prusiner, S. B. (1998) *Biochemistry 37*, 7185−7193.
35. Swietnicki, W., Petersen, R. B., Gambetti, P., and Surewicz, W. K. (1998) *J. Biol. Chem. 20*, 31048−31052.
36. Liemann, S., and Glockshuber, R. (1999) *Biochemistry 38*, 3258−3267.
37. Caughey, B., Raymond, G. J., Ernst, D., and Race, R. E. (1991) *J. Virol. 65*, 6597−6603.
38. Borchelt, D. R., Taraboulos, A., and Prusiner, S. B. (1992) *J. Biol. Chem. 267*, 16188−16199.
39. Turk, E., Teplow, D. B., Hood, L. E., and Prusiner, S. B. (1988) *Eur. J. Biochem. 176*, 21−30.
40. Somerville, R. A., Millson, G. C., and Kimberlin, R. H. (1980) *Intervirology 13*, 126−129.
41. Herrmann, L. M., and Caughey, B. (1998) *Neuroreport 9*, 2457−2461.
42. Kocisko, D. A., Come, J. H., Priola, S. A., Chesebro, B., Raymond, G. J., Lansbury, P. T., and Caughey, B. (1994) *Nature 370*, 471−474.
43. Horiuchi, M., and Caughey, B. (1999) *EMBO J. 18*, 3193−3203.

BI991967M